RESIDUAL SHEAR CAPACITY OF ASR DAMAGED REINFORCED CONCRETE BEAMS WITH RUPTURED STIRRUPS

Susumu Inoue[1*], Yasuhiro Mikata[1], Yuuki Takahashi[2], Katsuyuki Inamasu[3]

[1] Osaka Institute of Technology, Osaka, JAPAN

[2] Central Nippon Expressway Co. Ltd., Nagoya, JAPAN

[3] Hankyu Hanshin Building Management Co. Ltd., Osaka, JAPAN

Abstract

After the reports on the rupture of stirrups, as well as longitudinal steels, in T-shaped beams of bridge piers due to ASR expansion, vigorous research works have been done in Japan. From the view points of serviceability and structural safety, it is essential to make clear the shear resistant mechanism of ASR damaged members, in which stirrups are ruptured at their bent corners, in order to evaluate the residual shear capacity.

At the 13th ICAAR, the authors reported on the effect of rupture of stirrups on shear capacity of ASR damaged beams [1]. In that case, however, the observed ASR damage in the specimens was relatively small because of the short exposure period.

In this paper, the results of bond strength tests and beam loading tests after the exposure of more than 1100days, in this case ASR expansion almost finished, are reported. From the test results, residual shear capacity of ASR damaged reinforced concrete beams with ruptured stirrups is discussed.

Keywords: rupture of stirrups, shear capacity, ASR expansion, bond and anchorage characteristics, bond strength

1 INTRODUCTION

In recent years, it is reported in Japan that stirrups, as well as longitudinal steels, in T-shaped beams of bridge piers were ruptured at the bent corner or butt joints. In order to make clear the causes of this rupture, vigorous research works have been done after the finding of the rupture in existing reinforced concrete structures. Up to the present, it is recognized that this phenomenon occurred not only due to excessive ASR expansion but also under complex combinations of several factors, such as mechanical properties and surface shape of reinforcing bars, bending or welding methods of reinforcing bars, corrosive atmospheres and so on [2]. As for the load carrying capacity of ASR damaged structures, on the other hand, it is indicated that in most cases structural safety of damaged members is guaranteed at the present stage as far as the anchorage of ruptured steels is maintained by the bond between concrete and reinforcing bars based on the site inspections of the damaged structures as well as some experimental and analytical investigations. However, it is essential to make clear the shear resistant mechanism of ASR damaged members, in which stirrups are ruptured at their bent corners, in order to evaluate the residual shear capacity.

At the 13th ICAAR, the authors reported on the effect of rupture of stirrups on shear capacity of ASR damaged beams [1]. In that case, however, the discussions were mainly based on the test results of the

* Correspondence to : inoue@civil.oit.ac.jp

specimens with imitated ASR damage using expansive concrete. In addition, the observed damage in the specimens with practical ASR expansion was relatively small because of the short exposure period (approximately 500days).

In this paper, the results of bond strength tests and beam loading tests after the exposure of more than 1100days, in this case ASR expansion almost finished, are reported. From the test results, residual shear capacity of ASR damaged reinforced concrete beams with ruptured stirrups is discussed.

2 BOND STRENGTH TESTS

2.1 General

In order to evaluate the effects of rupture of stirrups on shear capacity of reinforced concrete members, it is essential to make clear the bond and anchorage characteristics of ruptured reinforcing bars embedded in ASR damaged concrete. Therefore, the bond strength tests were carried out in order to obtain fundamental data on bond and anchorage characteristics of ruptured steels.

2.2 Specimens

Specimens for the bond strength tests were concrete cubes of 100 x 100 x 100mm, in the center of which a reinforcing bar (length: 1000mm) was embedded as shown in Figure 1. Bond length of the embedded reinforcing bars was set as 5D (D: bar diameter). The rest part outside the bond length, the bond between concrete and reinforcing bar was eliminated by using grease and masking tape.

The main test variables were degree of ASR damage (exposure period) and diameter of reinforcing bars. Mix proportions of normal and ASR damaged concrete are listed in Table 1. Reactive fine and coarse aggregates, which are categorized as one of andesite and judged as “not harmless” by JIS A 1145 “Method of test for alkali-silica reactivity of aggregates by chemical method [3]”, were used in the pessimum (approximately 50% by weight) for the ASR damaged concrete. Sodium Chloride (NaCl) was also added so that the total alkali contents might become 8kg/m^3. This relatively high dosage of NaCl in the mix might have initiated corrosion of reinforcing bars. However, corrosion of the reinforcing bars was not discriminated after the loading tests.

Material properties of each concrete at the time of the bond strength test are listed in Table 2. Free expansion of the ASR concrete was about 0.31% at the age of 491 days and 0.44% at 1150 days respectively under the exposure in natural environment. In the ASR concrete specimens, expansive cracks were observed at the time of the bond strength tests. The maximum crack width in the ASR specimens after the exposure of 1150 days ranged from 0.40 to 1.10 mm, while 0.15-0.40 for the specimens after the exposure of 491 days.

As for the diameter of reinforcing bars, 10mm (D10) and 13mm (D13) were selected. Mechanical properties of these reinforcing bars are shown in Table 3.

Details of the specimens for the bond strength tests are listed in Table 4. The number of specimens for each combination of test variables is 3 for normal concrete, while 2 for ASR concrete after 491 days and 4 for ASR one after 1150 days, respectively.

2.3 Loading tests

Loading tests were carried out according to JSCE-G503 “Test method for bond strength between reinforcing steel and concrete by pull-out test” [4] as shown in Figure 2. During the loading tests, the applied loads and pull-out displacements were recorded. From these results, the average maximum bond stress as well as the stress at the pull-out displacement of 0.002D was calculated by using Equation 1.

$$\tau = \frac{\alpha P}{\pi L D} \tag{1}$$

where, τ : bond stress, P : applied load, L : bond length, D : bar diameter, α : modification factor considering the effect of compressive strength ($\alpha = 29.4 / f'_c$), f'_c : compressive strength at 28days (N/mm^2).

2.4 Results of the bond strength tests and discussions

In Table 4 are listed the average bond stress at the pull-out displacement of 0.002D, the maximum average bond stress and final failure mode. Some examples of the relationship between the average bond stress and pull-out displacement are also shown in Figure 3.

Failure mode

The observed failure modes of the specimens are divided mainly into two patterns, that is, 1) pull-out of reinforcing bar from the concrete, in which the applied load decreased gradually with increasing the pull-out displacement and 2) splitting failure of concrete due to the hoop tension generated by the bearing stress at the face of the lugs, which accompanied a sudden drop in load carrying capacity and a large increase of the pull-out displacement (See Figure 3). As listed in Table 4, the final failure mode of the normal concrete specimens was only the pull-out of reinforcing bar. In the ASR damaged concrete specimens, on the other hand, the observed failure mode was the splitting of concrete except for two specimens in which the reinforcing bar yielded before the bond failure. This implies that the pre-existing ASR cracks reduce the resistance against the hoop tension. However, the yielding of the reinforcing bar means that the bond strength was large enough in those specimens.

Average maximum bond stress

Figure 4 shows the relationship between the maximum average bond stress and the diameter of reinforcing bars. The maximum average bond stress in the ASR damaged concrete was larger than that of the normal concrete except for the case of D13 and exposure period of 491days, in which the crack density over 0.05mm was the largest. From these results, the maximum average bond stress in the ASR damaged concrete seems to be affected by the crack density of more than 0.05mm. However, significant deterioration in bond characteristics due to ASR could not be observed in this case except that the final failure mode tends to shift from pull-out of reinforcing bar to splitting of concrete due to the existence of expansive cracks. On the contrary, the authors' another tests on the bond strength of ASR damaged concrete (compressive strength: 28.4N/mm^2, elastic modulus: 8.5kN/mm^2, free expansion: 0.49%) [5] indicated that the reduction in the bond strength of the ASR damaged concrete became lager up to 25-36% compared with the normal concrete when the cover thickness is less than 4.5 times of the reinforcing bar. Therefore, further investigations should be necessary on the effects of cover thickness, bar diameter and so on in the different damage conditions, i.e. in the different crack densities in order to evaluate the bond characteristics of ruptured reinforcing bars in ASR damaged concrete.

3 BEAM LOADING TESTS

3.1 General

Residual load carrying capacity of ASR damaged concrete structures is affected by many factors, for examples, degree of ASR deterioration (expansion, cracks, etc.), magnitude of introduced chemical prestress and, of course, with or without rupture of longitudinal and/or shear reinforcement. Many of past researches indicated that reduction in load carrying capacity due to ASR is not so serious if an excessive expansion causing yielding or rupture of reinforcing bars did not occur. In addition, shear capacity of ASR damaged members becomes rather higher than that of non-damaged ones due to the introduced chemical prestress [6]. However, researches on residual load carrying capacity of ASR damaged members with ruptured stirrups and/or longitudinal steels scarcely exist at the present stage. The objectives of the beam loading tests are to investigate the effects of concrete expansion, rupture of stirrups and bond deterioration on shear capacity of reinforced concrete beams, and then to evaluate structural safety of ASR damaged members.

3.2 Specimens

In this test, totally six reinforced concrete beams with width x full depth x total length of 300 x 300 x 2000mm were used. Four of them were made by the same ASR concrete as used in the bond strength tests, while the other two was made by normal concrete. The mix proportions of these concrete are listed in Table 1. Five D19 reinforcing bars (f_{sy}=378N/mm^2, reinforcement ratio p=1.84%) were used for longitudinal reinforcement and D10 (f_{sy} =356 N/mm^2) stirrups were used for shear reinforcement. The spacing of stirrups was 120mm (p_w=0.40%), and the bent corners of these stirrups were cut in the tension side of the cross section in two of the four ASR concrete beams (the beams H-5, 6) as shown in Figure 5.

These beams were exposed to outside natural environment but off the ground for about 550 days (the beams N-1, H-1, 5) and 1150 days (the beams N-2, H-2, 6) after casting of concrete. During the exposure, they were simply supported and subjected to the stress caused by their dead load. The temperature range was -2.8 to 38.4 degree centigrade and the average was 16.2 degree centigrade, while the average relative humidity was about 60%. During the exposure, changes in the strain of concrete, longitudinal bars and stirrups were measured. Material properties of the normal and ASR concrete at the loading tests are shown in Table 5. The details of the tested beams are listed in Table 6. These beams were designed to fail in shear in order to evaluate the effectiveness of stirrups within ASR damaged concrete.

All of the beams were loaded monotonously up to failure under symmetrical two-point loads after the set exposure period. The shear span - effective depth ratio (a/d) was set as 2.0 so that the effect of shear force might become dominant. During the loading tests, applied load, deflections at the mid span and the loading points, changes of the strains in longitudinal steels and stirrups were recorded. In addition, the propagation of cracks during loading was observed.

3.3 Expansion characteristics of the ASR damaged beams

Figure 6 shows the expansive crack maps of the ASR damaged beams before the loading tests and Figure 7 shows the changes of the crack density over 0.05mm.

At the time of the loading tests, random cracks due to ASR expansion were observed in the ASR damaged beams especially in the upper side of them. As for the effect of the exposure period, the density of the expansive cracks became larger with increasing the exposure period as seen in Figure 6 and 7. As for the effect of the rupture of stirrups, longitudinal cracks along with the tensile reinforcing bars were observed in the beam H-5 and H-6 with ruptured stirrups. This implies that the restraining force against the expansion in the vertical direction was reduced in these beams, resulting in the concentration of crack opening along with the longitudinal bars. This was also the reason why the crack density over 0.05mm became smaller in the beams with ruptured stirrups compared at the same age.

As for the introduced chemical prestress in the ASR beams at the loading tests, the accurate values could not be obtained due to the breakage of the strain gages. However, the average restraining strain in the tensile reinforcing bars was approximately 0.0003 in the beam H-1 and 0.00055 in the beam H-5 at the age of 550 days. These values corresponded to the introduced chemical prestress at the tension fiber of 3.0N/mm^2

and 5.5N/mm^2, respectively. These values would become larger in the beams H-2 and H-6 at the age of 1150 days considering that the ASR expansion had not finished at the age of 550 days.

3.3 Results of the beam loading tests and discussions

Failure mode

In Table 6 is shown the summary of the loading tests. Figure 8 shows some examples of the final failure mode of the tested beams.

The normal concrete beam N-1 showed diagonal tension failure and the beam N-2 showed shear compression failure. These coincided with the predicted failure mode although the measured maximum loads were approximately 45% higher than the estimated shear capacity. This was mainly due to the conservativeness of the design shear equations in the JSCE Standard Specifications [7]. In the ASR damaged beams except for the beam H-6, on the other hand, flexural tension failure occurred although some cracks which had already existed before the loading tests extended to diagonal cracks with increasing the applied load. This increase in shear capacity is mainly due to the effect of introduced chemical prestress as indicated in the past researches. In the beams H-5 and H-6 with ruptured stirrups, however, shear bond cracks along with the tensile reinforcing bars were observed as seen in Figure 9. The ruptured stirrups could not effectively carry the dowel force of the main reinforcing bars at the diagonal cracks and this led to the development of the shear bond cracks, resulting in the brittle shear bond failure in the case of the beam H-6.

From these results, it is recognized that the effect of the introduced chemical prestress, which had a role to increase the concrete shear capacity, was rather larger than the negative effect of the deterioration of concrete in the case without the rupture of stirrups. However, the rupture of the stirrups in the tension zone of section might reduce the restraining effect against the dowel force of the main reinforcement at the diagonal cracks, resulting in the significant development of shear bond cracks.

Load - deflection relationship

Figure 10 shows the relationships between the applied load and the deflection at the loading point. As seen in this figure, the load carrying capacity of the normal beams N-1 and N-2 decreased abruptly after the maximum loads due to the shear failure, while the ASR beams which failed in flexure (H-1, 2 and 5) showed ductile load - deflection relationships. In the ASR damaged beam H-6, the load carrying capacity decreased abruptly due to the significant development of shear bond cracks.

Comparing among the ASR damaged beams, the flexural rigidity of the beams H-5 and H-6 after the applied load of about 300kN became somewhat smaller than those of the corresponding beams H-1 and H-2. This is mainly due to that the restraining effect of the ruptured stirrups against ASR expansion as well as the dowel force of the longitudinal reinforcements became smaller, resulting in the increase in crack width which caused the reduction of flexural rigidity.

As for the effect of the exposure period, the longer exposure period might cause the larger chemical prestress. The measured maximum loads of the beams H-2 and H-6 were larger than those of the corresponding beams H-1 and H-5 irrespective of the failure mode. This suggests that a larger amount of chemical prestress was introduced in these beams.

Stirrup strain

In Figure 11 are shown the relationships between the observed maximum stirrup strain and the applied load. As seen in this figure, the stirrup strain in the normal concrete beam N-1 began to increase after the diagonal cracking at about 250kN, and reached its yield strain at the final stage of loading. This implies that the truss mechanism was formed and the beam failed finally in shear due to the yielding of stirrups.

Almost the same tendency was observed in the normal concrete beam N-2 although the increasing ratio was small compared with the beam N-1 because of the formation of arch mechanism which led to the shear compression failure. In the ASR damaged beams, on the other hand, the stirrup strain began to increase at the larger applied loads compared with the normal concrete ones due to the introduced chemical prestress, and in most cases did not reach its yield strain even at the final stage of loading. This fact implies that the introduced chemical prestress increased the concrete shear capacity and restrained the opening of the diagonal cracks.

Comparing among the ASR damaged beams, however, the stirrup strains at the final stage of the beams H-5 and H-6 with ruptured stirrups was smaller than those of the corresponding beams H-1 and H-2. In the beams H-5 and H-6, shear bond cracks as seen in Figure 9 became significant with increasing the applied load. These bond cracks might occur due to the dowel force of the longitudinal bars, and the ruptured stirrups in the beams H-5 and H-6 could not restrain this force only by their bond to the concrete and consequently began to slip. This resulted in the smaller strains compared with those of the beams H-1 and H-2.

From the bond strength tests, the required bond length which guarantees the yielding of the stirrups was estimated approximately as 5D (=50mm, D: bar diameter), and Figure 11 shows that the ruptured stirrups worked well even in the case of the beam H-6 just before the shear bond failure due to the effect of the chemical prestress which increased the bond strength between concrete and stirrups.

4 CONCLUSIONS

In this study, the residual shear capacity of ASR damaged reinforced concrete beams with ruptured stirrups was investigated through the bond strength tests and beam loading tests after the exposure of 550 and 1150 days. The main conclusions obtained are summarized as follows.

1) The bond strength of the ASR damaged concrete after the exposure of 1150 days, of which the free expansive strain and the maximum crack width was 0.44 % and 1.10 mm respectively, scarcely decreased compared with that of the normal concrete due to the effect of introduced chemical prestress, although the final failure mode tended to become the splitting of concrete due to the existence of expansive cracks. However, these results were obtained from the restricted specimens and conditions. In addition, the bond strength of the ASR damaged concrete seemed to be affected by the expansive crack density over 0.05mm. Therefore, further investigations in the different expansion conditions are necessary, especially focussing on the effect of crack density.

2) The normal concrete beams failed finally in shear (N-1: diagonal tension failure, N-2: shear compression failure) as predicted. As for the ASR damaged beams, on the other hand, three (H-1, 2 and 5), of them failed in flexure even when the stirrups were ruptured (H-5), while the beam H-6 with ruptured stirrups after the exposure of 1150 days showed brittle shear bond failure. These results implied that the introduced chemical prestress due to ASR expansion increased the concrete shear capacity. This positive effect was rather larger compared with the negative effect of the deterioration in materials properties. As for the effects of the rupture of stirrups, the ruptured stirrups could not effectively restrain the ASR expansion in vertical direction and the dowel force of the longitudinal bars at the shear cracks, resulting in the significant propagation of the shear bond cracks along with the longitudinal bars. Such shear bond cracks might lead to the premature shear bond failure even when the ruptured stirrups carried some parts of the applied shear force just before the failure. Therefore, further investigations on the relationship between the outside damage profiles (cracking patterns, maximum crack width, crack density, etc) and the residual shear capacity are necessary to take rational countermeasures against the ASR damaged structures with ruptured stirrups.

5 REFERENCES

[1] Inoue, S, Oshita, H, Sawai, K, and Hatano, Y (2008): Effect of rupture of shear reinforcement on shear capacity of ASR damaged reinforced concrete beams. Proc. of the 13th ICAAR.

[2] Japan Society of Civil Engineers (2005): State-of-the-Art Report on the Countermeasures for the Damage Due to Alkali-Silica Reaction, Concrete Library 124 (in Japanese).

[3] Japanese Standards Association (2001): Method of test for alkali-silica reactivity of aggregates by chemical method, Japan Industrial Standards, JIS A 1145.

[4] Japan Society of Civil Engineers (2005): Testing method for bond strength between reinforcing steel and concrete by pull-out test, Standard Specifications for Concrete Structures-2005, Test Methods and Specifications, JSCE Standards, pp.239-242 (in Japanese).

[5] Takahashi Y., Sawai K., Mikata Y. and Inoue S. (2008): Effects of rupture of stirrups due to ASR on shear behavior of reinforced concrete beams, Proc. of the Japan Concrete Institute, Vol.30 (in Japanese).

[6] Inoue S., Fujii M., Kobayashi K. and Nakano K. (1989): Structural behaviours of reinforced concrete beams affected by Alkali-Silica Reaction, Proc. of the 8th ICAAR, pp.727-732.

[7] Japan Society of Civil Engineers (2002): Standard Specifications for Concrete Structures-2002, Structural Performance Verification.

Table 1: Mix proportions of used concrete

Type	G_{max} (mm)	Slump (cm)	Air (%)	W/C (%)	s/a (%)	Unit weight (kg/m³)							Water Reducing Agent (cc/m³)
						W	C	S_{normal}	$S_{reactive}$	G_{normal}	$G_{reactive}$	NaCl	
Normal	25	12	4.5	63	45.8	183	290	840	-	1080	-	-	726
ASR	25	12	4.5	63	45.8	183	290	394	411	507	492	13.1	726

Table 2: Properties of concrete (bond strength tests)

Type	Compressive strength f'_c (N/mm²)	Elastic modulus E_c (kN/mm²)	Free expansion (× 10^{-6})
Normal	28.2	24.9	-
ASR (491 days)	27.7	11.6	3100
ASR (1150 days)	26.5	25.4	4380

Table 3: Mechanical properties of reinforcing bars (bond strength tests)

Diameter	Yield strength f_{sy} (N/mm²)	Tensile strength f_{su} (N/mm²)	Elastic modulus E_s (kN/mm²)
D10	356	491	183
D13	333	488	189

Table 4: Details of specimens and results of tests (bond strength tests)

Specimen	Concrete type	Diameter of bars D (mm)	Bond length	Number of specimens	Maximum crack width (mm)	Crack density over 0.05mm (m/m²)	Average bond stress at 0.002D (N/mm²)	Maximum average bond stress (N/mm²)	Failure * mode
N-D10	Normal	10	5D	3	-	-	7.4	13.6	P:2, O:1
A-D10 (491 days)	ASR			2	0.3	12.1	9.2	17.2	S:2
A-D10 (1150 days)				4	1.1	14.1	13.1	16.1	S:2, Y:2
N-D13	Normal	13		3	-	-	7.9	14.6	P:3
A-D13 (491 days)	ASR			2	0.4	15.3	8.2	12.3	S:2
A-D13 (1150 days)				4	0.7	10.5	13.2	16.0	S:3, O:1

* P: pull-out of reinforcing bar, S: splitting failure of concrete, Y: yielding of bar, O: no data

Table 5: Properties of concrete of the beams specimens		
Type	Compressive Strength f'_c (N/mm²)	Elastic Modulus E_c (kN/mm²)
Normal (550 days)	27.4	22.4
Normal (1150 days)	28.2	24.9
ASR (550 days)	26.8	21.9
ASR (1150 days)	26.5	25.4

Table 6: Details of specimens and results of beam loading tests									
Specimens	Concrete	Rupture of Stirrups	Spacing of Stirrups (mm)	*1 P_u (kN)	*2 V_c (kN)	*3 V_s (kN)	*4 P_s (kN)	*5 P_{max} (kN)	*6 failure mode
N-1	Normal (550 days)	no	120	458	80.3	95.7	352	521	S
N-2	Normal (1150 days)			461	81.1	95.7	354	510	SC
H-1	ASR (550 days)			456	79.7	95.7	351	521	FT
H-2	ASR (1150 days)			456	79.4	95.7	350	615	FT
H-5	ASR (550 days)	yes		456	79.7	95.7	351	488	FT
H-6	ASR (1150 days)			456	79.4	95.7	350	576	SB

*1 calculated ultimate flexural capacity
*2 calculated shear capacity contributed by concrete (Based on JSCE Standard Specification [7])
In this case, the effect of chemical prestress is not considered.
*3 calculated shear capacity contributed by stirrups (Based on JSCE Standard Specification [7])
*4 calculated ultimate shear capacity ($P_s=2V_c+2V_s$)
*5 measured maximum load
*6 S: diagonal tension failure, SC: shear compression failure, FT: flexural tension failure, SB: shear bond failure

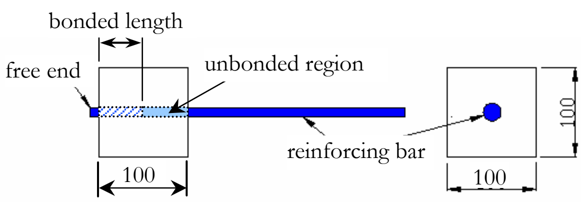

Figure 1: Test specimen for the bond strength tests

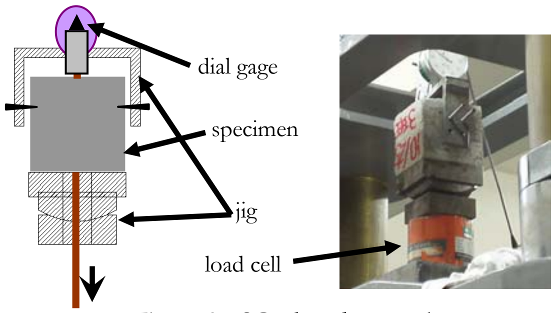

Figure 2: JSCE bond strength test

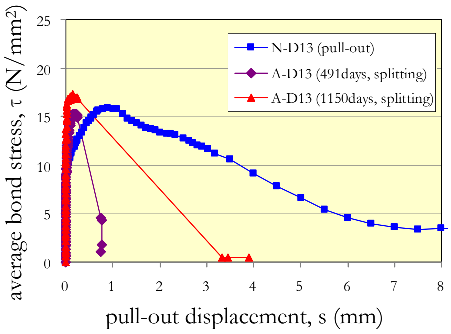

Figure 3: Examples of the relationship between the average bond stress and pull-out displacement

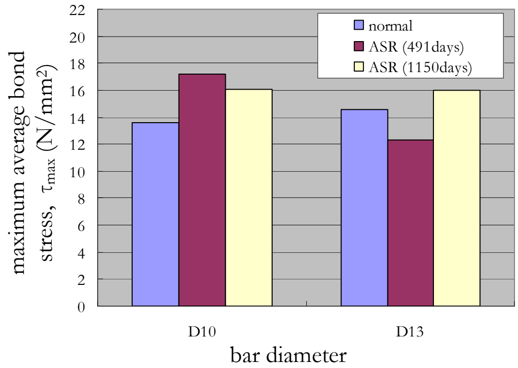

Figure 4: Relationship between the maximum average bond stress and the bar diameters

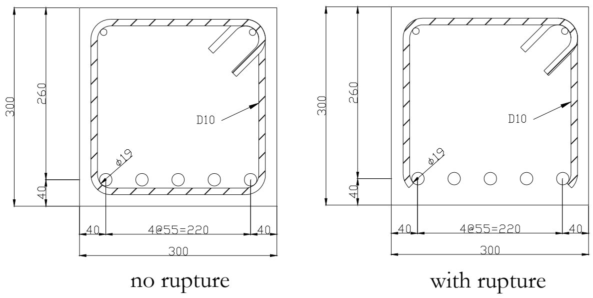

Figure 5: Cross sections of the tested beams

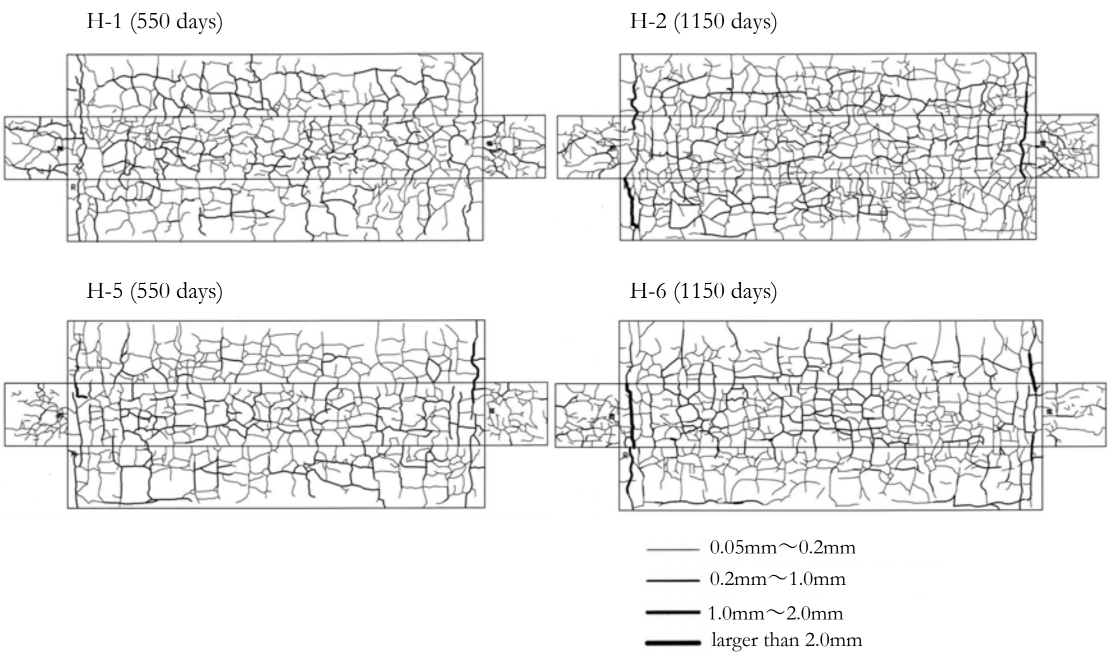

Figure 6: Crack maps of the ASR damaged beams

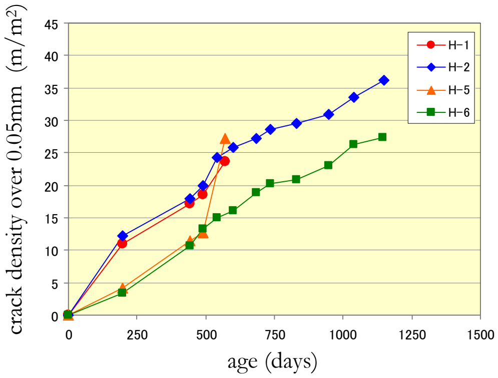

Figure 7: Crack density over 0.05mm

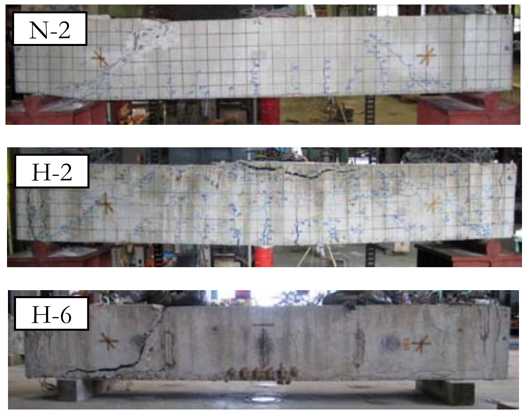

Figure 8: Examples of the final failure modes

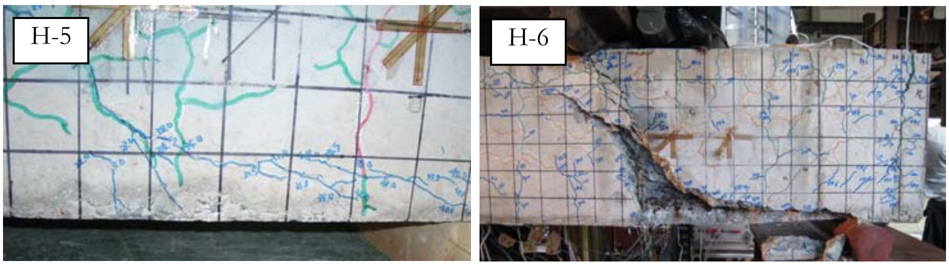

Figure 9: Observed shear bond cracks

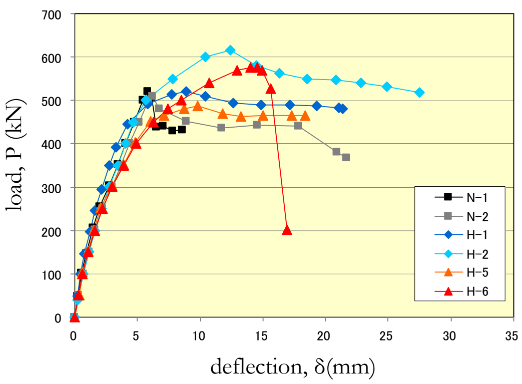

Figure 10: Relationship between the applied load and the deflection at the loading point

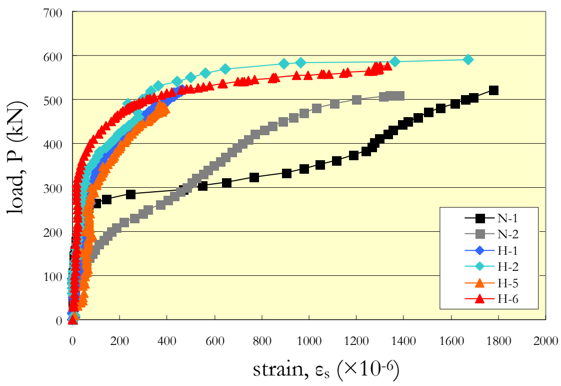

Figure 11: Relationship between stirrup strain and the applied load